J Herbmed Pharmacol. 2022; 11(3): 419-427.

http://www.herbmedpharmacol.com doi: 10.34172/jhp.2022.48

Journal of Herbmed Pharmacology

Antibacterial activity of airborne fungal mediated nanoparticles in combination with *Foeniculum vulgare* essential oil

Haitham Qaralleh[1*], Khaled Khleifat[2,3], Mouhamad Al-Limoun[3], Amjad Al-Tarawneh[4], Waqar Khleifat[3], Ibrahem Almajali[1], Rula Buqain[5], Khalid A. Shadid[6], Noorah Alsowayeh[7]

[1]Department of Medical Laboratory Sciences, Faculty of Science, Mutah University, Al-Karak, Jordan
[2]Faculty of Allied Medical Sciences, Al-Ahliyya Amman University, Amman, Jordan
[3]Biology Department, College of Science, Mutah University, Al-Karak, Jordan
[4]Prince Faisal Center for Dead Sea, Environmental and Energy Research, Mu'tah University, Jordan
[5]Cell Therapy Center, University of Jordan, Amman, Jordan
[6]Pharmacological and Diagnostic Research Center (PDRC), Faculty of Pharmacy, Al-Ahliyya Amman University, Amman 19328, Jordan
[7]Department of Biology, College of Education (Majmaah), Majmaah University, Al-Majmaah,11952, Saudi Arabia

ARTICLE INFO

Article Type:
Original Article

Article History:
Received: 17 March 2022
Accepted: 6 May 2022

Keywords:
Nanoparticles
Synergistic activity
Antimicrobial activity
Medicinal plant
Aspergillus flavus

ABSTRACT

Introduction: A cost-effective and ecologically friendly method of generating silver nanoparticles (AgNPs) includes pathways that utilize a variety of biological sources to decrease metal ions. This study was designed to synthesize AgNPs using a fungus strain *Aspergillus flavus* and evaluate its antibacterial activities alone or in combination with *Foeniculum vulgare* (fennel) essential oil (EO).

Methods: The antibacterial activity of different concentrations of biosynthesized AgNPs by *Aspergillus flavus* individually and in combination with fennel EO was investigated using disc diffusion methods and minimal inhibitory concentration (MIC). Bacterial species, including *Escherichia coli*, *Pseudomonas aeruginosa, Klebsiella pneumoniae*, *Enterobacter cloacae*, *Shigella* sp., *Staphylococcus aureus,* and *Staphylococcus epidermidis* were tested.

Results: Formation of dark brown color, ultraviolet-visible (UV/Vis) spectroscopy, transmission electron microscope (TEM), and attenuated total reflectance Fourier transform infrared spectroscopy (ATR-FTIR) were used for the characterization of AgNPs. Obvious synergistic effects were observed between AgNPs and EO of fennel (*F. vulgare*) with all tested bacteria except *S. aureus*, through increases in fold area of inhibition (IFAs) within the range of 0.15 to 8.87. Although *S. aureus* had the most susceptibility toward both AgNPs and EO of fennel (24 and 17 mm, respectively), no synergistic activity was exhibited. The best synergistic capacity resulted from AgNPs and fennel EO was observed against *S. epidermidis* (8.87-fold in IFA).

Conclusion: This study revealed that when biosynthesized AgNPs were mixed with the EO of *F. vulgare*, they became more bacteriostatic and might be developed to treat bacterial infections in the future.

Implication for health policy/practice/research/medical education:
These data may be used to develop and improve new antibacterial drugs as innovative medications by integrating nanoparticles (NPs) with antibiotics or other types of EOs of different plants.

Please cite this paper as: Qaralleh H, Khleifat K, Al-Limoun M, Al-Tarawneh A, Khleifat W, Almajali I, et al. Antibacterial activity of airborne fungal mediated nanoparticles in combination with *Foeniculum vulgare* essential oil. J Herbmed Pharmacol. 2022;11(3):419-427. doi: 10.34172/jhp.2022.48.

Introduction

Nanoscience is one of the most important branches of modern science, which deals with the knowledge, structure, and properties of nanoparticles and, at the same time, how these nanoparticles can be applied in all fields of science and technology (1). Therefore, nanoscience and its techniques are considered among the modern and active branches of the sciences. They are included

***Corresponding author**: Haitham Qaralleh,
Email: haitham@mutah.edu.jo

in many disciplines such as medicine, pharmacy, and engineering, but are almost in all fields (2).

The advancement of this field after obtaining many scientific research results in this regard has led to a radical change in the field of industry, whether from the beginning of the manufacture of raw materials or through the use of building blocks whose products are in nanoscales (3). Nanoparticles (NPs) have been described as a group of atoms containing at least one of the three outer dimensions with a size ranging from 1 to 100 nm (4,5). They usually exhibit several unique properties, whether physical or chemical, and of different sizes when matched with their bigger counterparts (6). The unique and new properties of NPs have been explored at the nano level and in a wide and varied field of possible applications, whether in medicine, pharmaceuticals, cosmetics, renewable energy, polymer industry, environmental treatment, water purification, and the manufacture of some medical devices (7).

The synthesis of NPs occurs in several ways, including chemical, physical, and biological fields. Among these methods are chemical methods, with some advantages, to produce them in large quantities and in a short time, while physical methods are quick by using radioactive materials as reducing agents without the need for toxic chemicals. However, chemical methods often include the use of some materials as helpers and stabilizers, which are toxic, therefore, do not lead to the production of non-environmental-friendly by-products. Moreover, the physical methods suffer from low production capacity coupled with high energy consumption and at the same time lead to unwanted nanoparticle size diversity and contamination of organic solvents (8-11). This synthetic approach is environmentally neutral, low cost, safe, non-toxic, and does not contain any harmful by-products. These biological, intracellular, and extracellular methods, which use bacterial, fungal, and plant cells or their extracts, are collectively called biosynthesis through green nanotechnology (12). Due to their nano size and high surface area, metal NPs exhibit unique and novel physical and chemical properties compared to their macroscale counterparts (13).

Among metal NPs, silver nanoparticles (AgNPs) are used in several fields, including medical, consumer, and healthcare products such as soaps, textile, plastics (14-16), and antimicrobial agents with wide spectrum activity against a variety of pathogenic bacteria and fungi (17-19). Multidrug-resistant bacteria is considered as a global concern, which have evolved as a result of excessive or insufficient antibiotic use (20). The emergence of these multidrug-resistant bacteria has been highlighted as a significant worldwide threat (21). In this situation, therefore, the combination of AgNPs with natural extracts may exhibit antibacterial synergies, resulting in the creation of a novel therapeutic method. Nanoparticle–antibiotic mixtures have been shown (*In vitro*) a reduction in the concentration of combined drugs toxicity and increasing antibacterial potential (22,23).

Foeniculum vulgare, commonly known as fennel, is an aromatic herb that is indigenous to the Mediterranean region but is cultivated in many countries. It has been used traditionally to treat a variety of diseases such as those related to the digestive, respiratory reproductive, and endocrine systems. It is also a galactagogue for nursing women (24). Badgujar et al (24) and Abou El-Soud et al (25) reported that it had antimicrobial, antioxidant, chemopreventive, antitumor, cytoprotective, hypoglycemic, hepatoprotective, and oestrogenic actions (24,25). Therefore, this study was designed to synthesize AgNPs using a fungus strain *Aspergillus flavus* and evaluate their antibacterial activities, alone or in combination with *F. vulgare* essential oil (EO) against various gram-negative and gram-positive bacteria.

Materials and Methods

Fungal strain

The airborne fungus was isolated from the warehouses of the Supplies Department at Mutah University by Dr. Amjad Al-Tarawneh from Prince Faisal Center for the Dead Sea, Environmental and Energy search at Mutah University, Jordan. By ITS sequencing, the fungus species was characterized as Aspergillus flavus (MACROGEN, Korea). A similarity search against the NCBI database was performed and then the sequence was deposited in the NCBI database (accession number MG973280.1).

Biosynthesis of AgNPs

The synthesis of AgNPs was prepared as described previously by Jaidev and Narasimha (26) with some modifications. Briefly, the fungal isolate was grown under aerobic conditions in a liquid culture medium at pH 7 by inoculating the liquid medium (100 mL) with 2.0×10^6 spores and then incubated, shaking at 150 rpm at 33˚C for 24 hours. After obtaining fungal biomass via filtering using (Whatman No. 1) filter paper, it was carefully cleaned with sterile and distilled water. Ten grams of wet biomass was placed in 100 mL of sterile deionized water and incubated at 33°C, pH 7.0, and agitated at 150 rpm for 48 hours. Then, the fungal filtrate was obtained by separating the fungal biomass from the suspension using filter paper (Whatman No. 1). To accomplish the biosynthesis process, AgNOs were added to the fungal filtrate (100 ml) at a concentration of 1 mM. The filtrate was then incubated in the dark for 24 hours at 33˚C and shaking rate of 150 rpm for 24 hours or as otherwise required.

Characterization of the synthesized AgNPs

The synthesized AgNPs were characterized using an ultraviolet-visible (UV/Vis) spectrophotometer,

transmission electron microscope (TEM), and attenuated total reflectance Fourier transform infrared spectroscopy (ATR-FTIR). To initially characterize the biosynthetic AgNPs, scanning UV/Vis light at the range (280-800 nm) was used. The same approach for the control flask was made but without AgNOs. TEM images of the synthesized AgNPs were captured by an FEI Versa 3D Dual Beam instrument (FEI, USA) and the AgNPs crystals were detected using MAXima-X XRD-7000 (SHIMADZU, Japan). The ATR-IR for the synthesized AgNPs was analyzed using a Bruker Alpha FTIR spectrometer (Bruker Optics GmbH, Ettlingen, Germany).

Plant material

Fresh *F. vulgare* leaves were collected in April and May in Irbid, southern Jordan. The plant was identified by Dr. Saleh Alquraan (Department of Biology, Mu'tah University, Al-Karak, Jordan). A voucher specimen (Bio202207) was deposited in the department of medical laboratory sciences, faculty of science, Mu'tah University, Al-Karak, Jordan. The fresh leaves were cleansed, dried, and crushed into a fine powder.

Extraction of essential oils

The EO components of *F. vulgare* leaves were extracted using a simple Clevenger apparatus. Briefly, a 50 g sample of ground plant material was hydro-distilled for three hours using simple Clevenger equipment. Diethyl ether was used to extract the EO from the aqueous phase. After evaporating the diethyl ether, anhydrous sodium sulfate was used to remove excess water. Finally, the extracted EO was refrigerated at 4°C for further investigation.

Bacterial species

Seven clinically isolated bacterial species were obtained from Al Bashir Hospital (Amman - Jordan). The bacterial strains tested included *E. coli, K. pneumonia, E. cloacae, Shigella sp.*, *P. aeruginosa, S. aureus,* and *S. epidermidis.* Clinical isolates were identified and confirm using bioMérieux VITEK® 2.

Preparation of bacterial suspension

The culture medium was prepared according to the standards of the Laboratory Standards Institute (CLSI M7-A7, 2012) (27). For this purpose, 1 CFU was selected and cultured in 5 mL nutrient broth (NB) and incubated overnight at 37°C, shaking at 150 rpm. Bacterial growth was set at 1.5×10^8 CFU/mL using 0.5 McFarland Standard.

Disc diffusion method

The antibacterial activities of EO and AgNPs solutions were investigated using disc diffusion assays described previously (28). This was carried out in Mueller-Hinton Agar containing Petri dishes. Disc diffusion tests were performed for the oil as described. Ready-made 6-mm paper discs laid on the agar surface were loaded with 5, 10, and 15 µL of EO. For AgNPs solution, discs laid on the agar surface were loaded with different volumes (5, 10, 15, 20, 40, and 60 µL), equal to 0.125, 0.25, 0.375, 0.5, 1, and 1.5 mg/mL, respectively. After 24 hours, the potential zone of inhibition for AgNPs doses and EO concentration against all bacterial samples were monitored and calculated (29).

Minimum inhibitory concentration (MIC)

MIC is defined as the lowest concentration of the tested materials needed to inhibit bacteria. Dilutions were prepared from a DMSO-EO stock solution to obtain 15, 10, 5, 2.5. 1.0, 0.5, and 0.25 mg/mL. For AgNPs solution, a series of volumes were made to obtain 60, 40, 20. 15, 10, 5, 2.0, 1.0, 0.5, and 0.25 µL, equal 1.5, 1, 0.5, 0.375, 0.25, 0.125, 0.05,0.025, 0.0125, and 0.00625 mg/mL for each, respectively. After 24 hours of incubation at 37°C, the concentration that showed no visible growth was reported as MIC (30,31).

Determination of the combined effect of AgNPs and fennel EO

The combination experiment of AgNPs and EO was performed using disc diffusion. Before determining the concentrations that were used in this experiment, 5, 10, and 15 µL of EO and 5, 10, 15, 20, 40, and 60 µL of AgNPs were used on each disc to be tested against seven bacterial species mentioned above. For studies on the synergy of combination between the two substances, each tested disc contained 5 µL of undiluted EO (5 µL per disc), and 5, 10, 15, 20 µL of AgNPs solution were used together (32). The synergistic effect was evaluated by using the IFA unit (increases in fold area). Positive combination activity was evidenced by an IFA of more than 0 and the synergistic possibility increases as the IFA increases (33). IFA was figured as shown in equation 1:

$$IFA = B^2 - A^2 / A^2$$

where A and B are the zones of inhibition (mm) produced by only EO or a combination of EO with AgNPs, respectively. When the inhibition value was zero, then the diameter of the disc was considered 6 mm for calculation purposes.

Statistical analysis

For all the experiments performed, the means and standard deviations of six independent tests were calculated. SPSS 22 was used to analyze the data (SPSS, Inc., USA). The significant differences were figured using the one-way analysis of variance (ANOVA), followed by Dunnett's post hoc test.

Results

Characterization of the synthesized AgNPs

The synthesized AgNPs were characterized using a UV-

Vis spectrophotometer, TEM, and ATR-IR. In Figure 1A, the UV–vis spectra revealed an SPR peak for AgNPs at 425 nm. The appearance of the intense dark brown color of the fungal filtrate arose after the addition of AgNOs, after a 24 hours time period (Figure 1B). The FTIR spectrum (Figure 2) showed a distinctive absorption band at 3400 cm^{-1} indicating the presence of OH groups. Absorption band at 2918 cm^{-1} suggested the presence of a C-H bond. The absorption band at 1650 cm^{-1} implied the existence of C-N and C-C bonds and the band at 1450 indicated the presence of N-H and C-N bonds. Additional characterization of AgNPs was confirmed using a TEM (Figure 3). Polydispersed NPs with an apparently spherical form were observed. Although some of these AgNPs appeared to be smaller or larger in size, most of their sizes ranged from 10 to 35 nm.

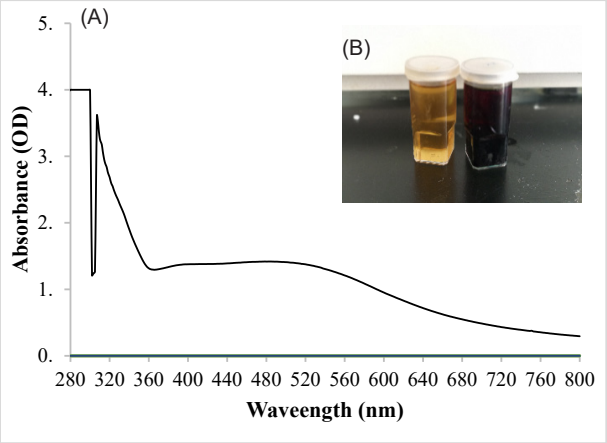

Figure 1. Ultraviolet-visible (UV/Vis) spectra (280-800 nm) for the synthesized silver nanoparticles (AgNPs) (A) and formation of dark brown color (B). AgNPs were prepared by adding 1 mM $AgNO_3$ to the fungal filtrate (100 mL) and incubating in the dark for 24 hours at 33°C with a shaking rate of 150 rpm for 24 hours. An UV/Vis spectrophotometer was used to confirm the formation of AgNPs in the range of 280–800 nm. The formation of a dark-brown color and the presence of an SPR peak at 425 nm indicated the formation of AgNPs.

Antibacterial effects of AgNPs and fennel EOs

Initially, the antibacterial effects of the AgNPs were evaluated using the disc diffusion method. This was performed by measuring the diameters of the inhibition zones produced by AgNPs against various pathogenic bacteria (Table 1). The AgNPs exhibited a broad-spectrum dose-dependent inhibitory effect against *K. pneumonia, E. coli*, *E. cloacae*, *S. aureus*, *S. epidermidis*, *Shigella* sp, and *P. aeruginosa,* with inhibition zones in the range of 7-24 mm. At the highest concentration tested (1.50 mg/mL), the gram-positive strains tested (*S. aureus* and *S. epidermidis*) were the most susceptible strains with inhibition zones of 24 and 20 mm, respectively. In contrast, the gram-negative strains were less susceptible to AgNPs since the maximum inhibition zone observed was 18 mm against *Shigella* sp. *P. aeruginosa* was the most resistant strain tested (10 mm). To confirm the antibacterial activity, the MIC of AgNPs was determined. As shown in Table 2, AgNPs showed bacteriostatic activities against *E. cloacae* and *K. pneumonia* with MIC value of 0.025 mg/mL, followed by *S. epidermidis* (0.05 mg/mL), *E. coli* and *Shigella sp.* (0.075 mg/mL), *S. aureus* (0.10 mg/mL), and *P. aeruginosa* (0.125 mg/mL).

Disc diffusion method, as well as MIC values, were applied here to investigate the antibacterial activity of fennel EOs. As shown in Table 3, the broad-spectrum antibacterial activity of fennel EOs was observed. Strong antibacterial activity was observed against all strains tested in a dose-dependent manner. At the highest concentration tested, the maximum inhibition zones observed were 17 mm against *K. pneumonia, E. coli,* and *S. aureus* followed by *E. cloacae* and *P. aeruginosa* (16 mm), and *S. epidermidis* and *Shigella sp.* (15 mm). The MIC values of the fennel EOs were parallel to the size of the inhibition zones (Table 2). The lowest MIC value for the fennel EO observed was 1.25 mg/mL against *E. coli* followed by *S. aureus* and *K. pneumoniae* (2.5 mg/mL, each) and *Shigella* sp (5.0 mg/mL). The MIC value of 7.5

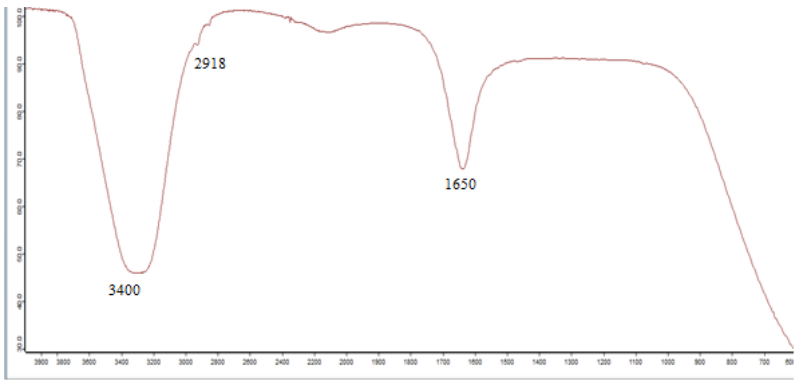

Figure 2. Attenuated total reflectance Fourier transform infrared spectroscopy (ATR-FTIR) analysis of silver nanoparticles (AgNPs). A portion of the synthesized AgNPs was analyzed using ATR-IR. The result showed the presence of absorption bands at 3400, 2918, and 1650 cm^{-1}, which suggested the presence of a C-H bond, C-N and C-C bonds and N-H and C-N bonds, respectively.

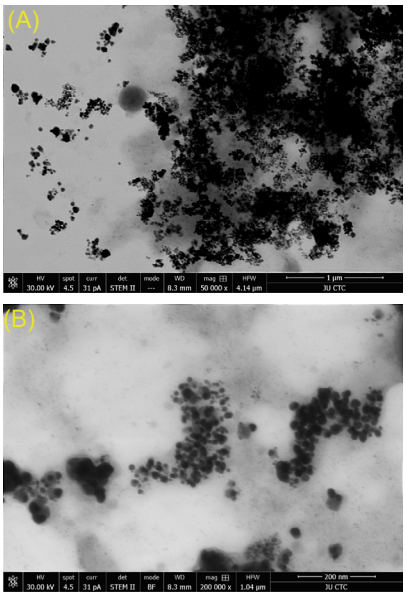

Figure 3. Transmission electron microscope (TEM) micrograph of silver nanoparticles (AgNPs). (A: 1 µm and B: 200 nm). A portion of the synthesized AgNPs was analyzed using TEM. The results showed that AgNPs were spherical in shape and polydispersed, but most of their sizes ranged from 10 to 35 nm.

mg/mL was reported for the fennel EO against *E. cloacae, P. aeruginosa,* and *S. epidermidis.* Overall, the results of the inhibition zones, as well as the MIC values, indicated a broad-spectrum antibacterial action for the fennel EOs.

Synergistic effects of AgNPs and fennel EOs against different bacteria strains

Even though the inhibition zones analysis revealed susceptibility to all AgNPs concentrations utilized for all bacterial samples, only 0.125, 0.250, 0.375, and 0.5 mg/mL of AgNPs were combined with the minimum concentration (5 µL) of EO (Table 4). However, a synergetic effect was found when 5 µg/mL EO was tested in combination against *K. pneumoniae* with the 0.125, 0.250, 0.375, and 0.5 mg/mL of AgNPs with IFA values of 3.45, 3.93, 4.4, and 4.98, respectively. The synergistic effects of the combination of AgNPs and EO of fennel against *E. coli* showed a wide variation (Table 4). When the different concentrations of AgNPs (0.125, 0.250, 0.375, and 0.5 mg/mL) were combined with 5 µL of EO of fennel, the AgNPs produced appreciable synergy depicted by the increases in the IFA 0.474, 0.653, 1.040, and 2.19, respectively. The concentrations of AgNPs (0.125, 0.250, 0.375, 0.5, 1, and 1.5 mg/mL) used alone led to the inhibition zone of 9, 10, 11, 12, 13, and 14 mm, respectively. The 20 µL of AgNPs showed significant effects (IFAs of 2.19) in the presence of 5 µL of EO when used against *E. coli*. The effect of combined AgNPs and EO against *E. cloacae*, the antibacterial effect of AgNPs showed significant synergism ranging from 0.15 to 0.84 IFA (Table 4). There were similar responses of the bacteria using the different combinations of fennel EO in addition to AgNPs. Using different concentrations of AgNPs and EO of fennel against *Shigella* sp., the inhibition zones were obtained in a concentration-dependent manner (Tables 1 and 2). When combining different concentrations of AgNPs with 5 µl of fennel EO, it led to a clear increase in the inhibition zones, which was expressed by an increase in the fold area of inhibition (IFA), ranging from 0.15 to 1.37 (Table 4).

The combination of EO with AgNPs produced varied degrees of the enhancement of antimicrobial effect against

Table 2. Minimum Inhibitory Concentration (MIC) of biosynthesized silver nanoparticles (AgNP) (mm) against different bacteria

Bacteria	MIC (mg/mL)	
	AgNPs	Essential oil
E. coli	0.075	1.25
E. cloacae	0.025	7.5
Shigella sp.	0.075	5.0
P. aeruginosa	>0.125	7.5
K. pneumonia	0.025	2.5
S. epidermidis	0.05	7.5
S. aureus	0.10	2.5

Data are expressed as mean of triplicates. The MICs of the biosynthesized AgNPs and the EO of fennel were determined using the microdilution method. The results showed that AgNPs possess bacteriostatic activity at concentrations ranging from 0.025 to 0.125 mg/mL, whereas the EO of fennel was bacteriostatic at concentrations ranging from 1.25 to 7.5 mg/mL.

Table 1. Inhibition zones of different concentrations of biosynthesized silver nanoparticles (AgNPs) (mg/mL) by *Aspergillus flavus*

AgNPs concentration (mg/mL)	*K. pneumonia*	*E. coli*	*E. cloacae*	*Shigella sp.*	*P. aeruginosa*	*S. aureus*	*S. epidermidis*
	Inhibition zone (mm)						
0.125	9.17 ± 0.3	9.0 ± 0.5	9.0 ± 0.5	9.0 ± 0.5	7.0 ± 0.0	9.0 ± 0.0	8.0 ± 0.0
0.25	10.33 ± 0.3	10.0 ± 0.0	10.0 ± 0.0	11.0 ± 0.0	7.0 ± 0.0	11.5 ± 0.5	9.0 ± 0.0
0.375	11.0 ± 0.5	11.17 ± 0.3	12.33 ± 0.3	12.0 ± 0.0	7.0 ± 0.0	12.17 ± 0.3	11.33 ± 0.3
0.50	13.0 ± 0.5	12.0 ± 0.0	13.33 ± 0.3	14.0 ± 0.0	8.0 ± 0.0	19.0 ± 0.0	12.17 ± 0.3
1.0	14.0 ± 0.0	13.0 ± 0.0	16.0 ± 0.0	15.0 ± 0.0	9.3 ± 0.3	22.5 ± 0.5	1.04 ± 0.0
1.50	17.0 ± 0.5	14.0 ± 0.0	20.0 ± 0.3	18.0 ± 0.0	10.5 ± 0.3	24.0 ± 0.0	15.0 ± 0.0

Data are expressed as mean ± SD of triplicates. Disc diffusion method was used to evaluate the antibacterial activity of AgNPs at concentrations equal to 0.123, 0.25, 0.375, 0.50, 1.1, and 1.50 mg/mL. AgNPs exhibited a broad-spectrum dose-dependent inhibitory effect against *K. pneumonia, E. coli, E. cloacae, S. aureus, S. epidermidis, Shigella sp,* and *P. aeruginosa.*

Table 3. Inhibition zones of different concentrations of essential oil (EO) of fennel (µL)

EO concentration (µL	*K. pneumonia*	*E. coli*	*E. cloacae*	*Shigella sp.*	*P. aeruginosa*	*S. aureus*	*S. epidermidis*
	Inhibition zone (mm)						
5	9.0±0.0	14.17±0.3	13.0±0.0	13.3±0.3	14.0±0.0	13.0±0.0	7.0±0.0
10	15.5±0.3	15.0±0.0	14.0±0.0	14.5±0.5	15.3±0.3	15.0±0.3	13.0±0.0
15	17.0±0.0	17.0±0.0	16.0±0.0	15.0±0.0	16.3±0.3	17.3±0.3	15.0±0.5

Data are expressed as mean±SD of triplicates. Disc diffusion method was used to evaluate the antibacterial activity of AgNPs. Fennel EOs exhibited a broad-spectrum dose-dependent inhibitory effect against the above bacteria.

P aeruginosa. Based on IFA measurements, the synergistic results were 0.30, 0.91, 1.113, and 1.36 for 0.125, 0.250, 0.375, and 0.5 mg/mL AgNPs concentrations, respectively (Table 3). However, all concentrations of AgNPs and 5 µL of EO exhibited reasonable susceptibility against *P. aeruginosa*, with significant inhibition zones ranging between 16 and 20 mm. The synergistic effects of these two components against *P. aeruginosa* were significant in comparison with other bacterial species tested in this study. The effects of EO and NPs individually were relatively low. For example, at 5 µl EO and 0.5 mg/mL NPs, the inhibition zones were 14 and 8 mm, respectively, while the synergy result between the two volumes used was 20 mm and IFA of 1.36.

Table 4. Synergistic effect of AgNPs and EO of fennel against different bacteria

	AgNPs (µL)	AgNPs + EO (mm)*	IFA
K. pneumonia	5	19.0 ± 0.5	3.5
	10	20.0 ± 0.3	3.9
	15	21.5 ± 0.5	4.7
	20	22.0 ± 0.0	5.0
E. coli	5	17.5 ± 0.0	2.8
	10	18.0 ± 0.0	3.0
	15	20.3 ± 0.3	4.1
	20	25.0+0.0	6.7
E. cloacae	5	15.0 ± 0.0	1.8
	10	17.0 ± 0.5	2.6
	15	18.0 ± 0.5	3.0
	20	19.0 ± 0.5	3.5
Shigella sp.	5	14.0 ± 0.0	0.0
	10	16.0 ± 0.0	0.0
	15	17.0 ± 0.0	0.2
	20	20.5 ± 0.5	0.6
P. aeruginosa	5	16.0 ± 0.5	1.4
	10	18.0 ± 0.5	3.0
	15	19.0 ± 0.5	4.4
	20	20.5 ± 0.5	5.0
S. aureus	5	7.0 ± 0.0	1.4
	10	9.0 ± 0.0	2.2
	15	10.0 ± 0.5	2.6
	20	11.5 ± 0.5	4.2
S. epidermidis	5	14.0 ± 0.0	2.2
	10	18.0 ± 0.5	3.0
	15	21.0 ± 0.0	3.5
	20	22.0 ± 0.5	4.2

Data are expressed as mean±SD of triplicates. The synergistic effect between silver nanoparticles (AgNPs) and EO was performed using disc diffusion at concentrations equal to 5, 10, 15, 20 µL of AgNPs solution and 5 µL of undiluted EO (5 µL per disc). After 24 h of incubation at 37°C, the inhibition zones were measured, and the increase in the fold area (IFA) was calculated using this equation: $IFA = B^2 - A^2 / A^2$, where A and B are the zones of inhibition (mm) produced by only EO or a combination of EO with AgNPs, respectively. Positive combination activity was evidenced by an IFA of more than 0, and the synergistic possibility increases as the IFA increases. There was a synergistic effect between AgNPs and EO against all strains tested except *Shigella* sp.

Although *S. aureus* was highly sensitive to all concentrations of fennel EO and AgNPs, however, when using their combinations, no synergistic result was shown in contrast to *S. epidermidis*. *S. epidermidis* cells, unlike *S. aureus,* have shown their sensitivity to all concentrations of EO and AgNPs alone or in combination. The acquired findings prove the synergistic action of AgNPs and EOs. The resulted IFAs from these combinations were 14, 18, 21, and 22 for 0.125, 0.250, 0.375, and 0.5 mg/mL of AgNPs, respectively. Indeed, the findings strongly indicate that when AgNPs were employed in conjunction with EOs, the necessary concentrations of AgNPs are significantly reduced for all bacterial strains examined.

Discussion

Biological exploration in different and less available conditions has allowed us to study and analyze microbial diversity and confront specialized microbes through the production of biological sourced compounds, such as metal NPs. When comparing the microorganisms' dependent biosynthesis of AgNPs with chemical and physical methods, the manufacture of AgNPs by microorganisms, particularly fungus, is more cost-effective, environmentally friendly, and does not require the use of any hazardous chemicals (34). In this study, an airborne fungal strain was isolated and identified, and its biological ability was revealed to be competent for AgNP biosynthesis. Previous research on several types of EOs established their synergy with a wide variety of available commercial antibiotics and the efficacy of these combinations by allowing for the introduction of novel therapeutic application techniques (32,35). In this study, a new strategic approach was investigated through the possibility of synergizing the EO of fennel (*F. vulgare*) and AgNPs biologically synthesized by the isolated air-born fungus *A. flavus*.

Depending on the primary diagnostic methods, the appearance of the intense dark brown color of the fungal filtrate arose after the addition of AgNOs, over a 24 h time period. The observed color change was due to the deposited AgNPs' surface plasmon resonance (SPR) (26,36). In Figure 2, the UV–vis spectra revealed an SPR peak for AgNPs at 425 nm. The size and structure of AgNPs are well recognized to reflect the absorbance peak (37,38). The exact mechanism of AgNP synthesis by fungi is still not elucidated, but a previous research indicated that the nitrate reduction process depended on the nitrate reductase-dependent NADH, which are important agents for the biosynthesis of AgNPs (30).

In this study, the gram-negative strains were less susceptible to AgNPs. It has been reported that variations in the responses to NPs could be due to differences in cell surface components between gram-negative and gram-positive bacteria (26,39,40). AgNPs' catalytic activity and other features, including their antibacterial actions, are dependent on their unique surface areas. With an increase in the specific surface area of NPs, their biological effectiveness increases as a result of an increase in surface energy (32). AgNPs are highly toxic to microorganisms because of their highly reactive component species and their large surface areas (41).

Despite the difficulty of describing medicinal plants as antimicrobials, the EO of fennel is widely used and is considered one of the components of some medicines that are used to treat the respiratory system. However, this plant is commonly used as one of the ingredients of spices that are added to food (25). Our data indicate the great potential of fennel EO as a promising gram-negative and gram-positive antibacterial therapy (Table 2). As a result, this study reveals the importance of fennel EO in controlling resistant bacteria, as shown in Tables 2 and 3. Moreover, the plant fennel EO was effective against antibiotic-resistant bacteria at very low concentrations (5 µL), thus reducing potential toxic effects.

The mechanism of antibacterial action of combinations is significantly different from the action mechanism of the same AgNPs or EO when used alone. The antibiotic cefixime's action against *K. pneumonia* was boosted by 26% when combined with *Centaurea damascena* EO (28,35). Our findings indicate that 5 µL of *F. vulgare* EO has an effect on the AgNPs' antibacterial activity and might even be employed as a possible adjuvant in the treatment of pneumonia caused by *K. pneumonia*. As a result, the effect indicated in this circumstance is due to the combination of EO and AgNPs. Microorganisms are supposed to have a negative charge, whereas metal oxides have a positive charge (42). This attracts the microorganism to the treated surface via an "electrostatic" force. While contact is established, the microorganism is rapidly oxidized and dies. In general, it is hypothesized that NPs discharge ions that react with the bacterial protein thiol group on the surface. These proteins emerge through the membrane of the bacterial cell, facilitating nutrients to be transported through the cell wall. NPs inactivate these proteins, reducing the permeability character of the membrane thus eventually ending in cell death (42).

Overall, the AgNPs showed different levels of inhibition against all tested bacteria. Accordingly, AgNPs can be included in different combinations with multiple compounds with new techniques that treat bacterial resistance to many antibiotics. However, the relationship between the bactericidal strength of AgNPs and their concentrations is related to the bacterial species (43). Just as reported in previous investigations (44), *P. aeruginosa* was less affected than *E. coli* by AgNPs. The inhibitory region of *S. aureus* was more pronounced than that of *E. coli* and *S. epidermis*. It was discovered that Gram-positive and gram-negative bacteria exhibit differential sensitivity to AgNPs, perhaps due to variations in their membranes and cell walls (45). Although the concentration of the EO was doubled from 5 to 10 to 15 µL, the inhibitory effects of EO on bacterial growth were concentration-dependent manner. However, this increase in concentration was mostly not reflected in the results related to the IFs. This reflects that the amount of active substance present in 10 µL of oil is sufficient, instead of 5 µL or 15 µL, because increasing the concentration from 10 to 15 µL *found not* to *significantly* influence the increase of the diameter of the inhibition zone.

Conclusion

The findings of this study show that fungal-mediated AgNPs could be employed to manage bacterial infections. Furthermore, infections caused by resistant strains can be treated using both nontoxic AgNPs and drug of choice antibiotics. More research is needed to establish the synergistic effect of these combinations and their mechanisms of action.

Authors' contribution

KhKh, AM, and QH conceived and designed the study, KhW and BR carried out the experiments, AA, AI, ShKh, and AN participated in the study design and performed the statistical analysis. All authors participated in the manuscript writing and approved the final manuscript for publication.

Conflict of interests

The authors declare no conflict of interest.

Ethical considerations

Ethical issues (including plagiarism, data fabrication, double publication and etc) have been completely observed by the authors.

Funding/Support

This research was supported by the Deanship of Scientific Research at Mutah University, Jordan (Projects No. 388/2021 and 347/2020).

References

1. Satalkar P, Elger BS, Shaw DM. Defining nano, nanotechnology and nanomedicine: why should it matter? Sci Eng Ethics. 2016;22(5):1255-76. doi: 10.1007/s11948-015-9705-6.
2. Sergeev GB, Shabatina TI. Cryochemistry of nanometals. Colloids Surf A Physicochem Eng Asp. 2008;313-314:18-22. doi: 10.1016/j.colsurfa.2007.04.064.
3. Ramamurthy CH, Sampath KS, Arunkumar P, Kumar MS, Sujatha V, Premkumar K, et al. Green synthesis and characterization of selenium nanoparticles and its augmented cytotoxicity with doxorubicin on cancer cells. Bioprocess Biosyst Eng. 2013;36(8):1131-9. doi: 10.1007/s00449-012-0867-1.
4. Calderón-Jiménez B, Johnson ME, Montoro Bustos AR, Murphy KE, Winchester MR, Vega Baudrit JR. Silver nanoparticles: technological advances, societal impacts, and metrological challenges. Front Chem. 2017;5:6. doi: 10.3389/fchem.2017.00006.
5. Williams D. The relationship between biomaterials and nanotechnology. Biomaterials. 2008;29(12):1737-8. doi: 10.1016/j.biomaterials.2008.01.003.
6. Colvin VL, Schlamp MC, Alivisatos AP. Light-emitting diodes made from cadmium selenide nanocrystals and a semiconducting polymer. Nature. 1994;370(6488):354-7. doi: 10.1038/370354a0.
7. Xu ZP, Zeng QH, Lu GQ, Yu AB. Inorganic nanoparticles as carriers for efficient cellular delivery. Chem Eng Sci. 2006;61(3):1027-40. doi: 10.1016/j.ces.2005.06.019.
8. Mafuné F, Kohno JY, Takeda Y, Kondow T, Sawabe H. Formation of gold nanoparticles by laser ablation in aqueous solution of surfactant. J Phys Chem B. 2001;105(22):5114-20. doi: 10.1021/jp0037091.
9. Kabashin AV, Meunier M. Synthesis of colloidal nanoparticles during femtosecond laser ablation of gold in water. J Appl Phys. 2003;94(12):7941-3. doi: 10.1063/1.1626793.
10. Sylvestre JP, Kabashin AV, Sacher E, Meunier M, Luong JH. Stabilization and size control of gold nanoparticles during laser ablation in aqueous cyclodextrins. J Am Chem Soc. 2004;126(23):7176-7. doi: 10.1021/ja048678s.
11. Hamidia Z, Shahanipour K, Talebian N, Monajemi R. Preparation of chelidonine highly loaded poly (lactide-co-glycolide)-based nanoparticles using a single emulsion method: cytotoxic effect on MDA-MB-231 cell line. J Herbmed Pharmacol. 2021;11(1):114-20. doi: 10.34172/jhp.2022.13.
12. Klaus T, Joerger R, Olsson E, Granqvist CG. Silver-based crystalline nanoparticles, microbially fabricated. Proc Natl Acad Sci U S A. 1999;96(24):13611-4. doi: 10.1073/pnas.96.24.13611.
13. Gentile A, Ruffino F, Grimaldi MG. Complex-morphology metal-based nanostructures: fabrication, characterization, and applications. Nanomaterials (Basel). 2016;6(6):110. doi: 10.3390/nano6060110.
14. Hossain MK, Drmosh QA, Yamani ZH, Tabet N. Silver nanoparticles on zinc oxide thin film: an insight in fabrication and characterization. IOP Conf Ser Mater Sci Eng. 2014;64:012018. doi: 10.1088/1757-899x/64/1/012018.
15. Fabrega J, Luoma SN, Tyler CR, Galloway TS, Lead JR. Silver nanoparticles: behaviour and effects in the aquatic environment. Environ Int. 2011;37(2):517-31. doi: 10.1016/j.envint.2010.10.012.
16. Dallas P, Sharma VK, Zboril R. Silver polymeric nanocomposites as advanced antimicrobial agents: classification, synthetic paths, applications, and perspectives. Adv Colloid Interface Sci. 2011;166(1-2):119-35. doi: 10.1016/j.cis.2011.05.008.
17. Bhakya S, Muthukrishnan S, Sukumaran M, Muthukumar M. Biogenic synthesis of silver nanoparticles and their antioxidant and antibacterial activity. Appl Nanosci. 2016;6(5):755-66. doi: 10.1007/s13204-015-0473-z.
18. Jesudoss SK, Vijaya JJ, Kennedy LJ, Rajan PI, Al-Lohedan HA, Ramalingam RJ, et al. Studies on the efficient dual performance of Mn1-xNixFe2O4 spinel nanoparticles in photodegradation and antibacterial activity. J Photochem Photobiol B. 2016;165:121-32. doi: 10.1016/j.jphotobiol.2016.10.004.
19. Barabadi H, Honary S, Ali Mohammadi M, Ahmadpour E, Rahimi MT, Alizadeh A, et al. Green chemical synthesis of gold nanoparticles by using *Penicillium aculeatum* and their scolicidal activity against hydatid cyst protoscolices of *Echinococcus granulosus*. Environ Sci Pollut Res Int. 2017;24(6):5800-10. doi: 10.1007/s11356-016-8291-8.
20. Anandan M, Poorani G, Boomi P, Varunkumar K, Anand K, Chuturgoon AA, et al. Green synthesis of anisotropic silver nanoparticles from the aqueous leaf extract of *Dodonaea viscosa* with their antibacterial and anticancer activities. Process Biochem. 2019;80:80-8. doi: 10.1016/j.procbio.2019.02.014.
21. Jeyaraj M, Sathishkumar G, Sivanandhan G, MubarakAli D, Rajesh M, Arun R, et al. Biogenic silver nanoparticles for cancer treatment: an experimental report. Colloids Surf B Biointerfaces. 2013;106:86-92. doi: 10.1016/j.colsurfb.2013.01.027.
22. Saravanan M, Barik SK, MubarakAli D, Prakash P, Pugazhendhi A. Synthesis of silver nanoparticles from *Bacillus brevis* (NCIM 2533) and their antibacterial activity against pathogenic bacteria. Microb Pathog. 2018;116:221-6. doi: 10.1016/j.micpath.2018.01.038.
23. ALrawashdeh I, Qaralleh H, Al-Limoun MO, Khleifat KM. Antibactrial activity of *Asteriscus graveolens* methanolic extract: synergistic effect with fungal mediated nanoparticles against some enteric bacterial human pathogens. J Basic Appl Res Biomed. 2019;5(2):89-98. doi: 10.51152/jbarbiomed.v5i2.40.
24. Badgujar SB, Patel VV, Bandivdekar AH. *Foeniculum vulgare* Mill: a review of its botany, phytochemistry, pharmacology, contemporary application, and toxicology. Biomed Res Int. 2014;2014:842674. doi: 10.1155/2014/842674.
25. Abou El-Soud N, El-Laithy N, El-Saeed G, Wahby M, Khalil M, Morsy F, et al. Antidiabetic activities of *Foeniculum vulgare* Mill. essential oil in streptozotocin-induced diabetic rats. Maced J Med Sci. 2011;4(2):139-46.

doi: 10.3889/mjms.1857-5773.2011.0173.
26. Jaidev LR, Narasimha G. Fungal mediated biosynthesis of silver nanoparticles, characterization and antimicrobial activity. Colloids Surf B Biointerfaces. 2010;81(2):430-3. doi: 10.1016/j.colsurfb.2010.07.033.
27. Clinical and Laboratory Standards Institute (CLSI). Methods for Dilution Antimicrobial Susceptibility Tests for Bacteria That Grow Aerobically; Approved Standard. Doc CLSI M7-A7. Wayne, PA: CLSI; 2012.
28. Qaralleh H, Khleifat KM, Al-Limoun MO, Alzedaneen FY, Al-Tawarah N. Antibacterial and synergistic effect of biosynthesized silver nanoparticles using the fungi *Tritirachium oryzae* W5H with essential oil of *Centaurea damascena* to enhance conventional antibiotics activity. Adv Nat Sci Nanosci Nanotechnol. 2019;10(2):025016. doi: 10.1088/2043-6254/ab2867.
29. Essiet GA, Anwankwo MU, Akuodor GC, Ajoku GA, Offor CC, Megwas AU, et al. Antibacterial and toxicological evaluation of the ethanol leaf extract of *Anthonotha macrophylla*. J Herbmed Pharmacol. 2019;8(3):205-11. doi: 10.15171/jhp.2019.30.
30. Al-Limoun MO, Qaralleh H, Khleifat KM, Al-Anber M, Al-Tarawneh A, Al-Sharafa K, et al. Culture media composition and reduction potential optimization of mycelia-free filtrate for the biosynthesis of silver nanoparticles using the fungus *Tritirachium oryzae* W5H. Curr Nanosci. 2020;16(5):757-69. doi: 10.2174/1573413715666190725111956.
31. Simamora A, Santoso AW, Rahayu I, Timotius KH. Enzyme inhibitory, antioxidant, and antibacterial activities of ethanol fruit extract of *Muntingia calabura* Linn. J Herbmed Pharmacol. 2020;9(4):346-54. doi: 10.34172/jhp.2020.44.
32. Khlaifat AM, Al-Limoun MO, Khleifat KM, Al Tarawneh AA, Qaralleh H, Rayyan EA, et al. Antibacterial synergy of *Tritirachium oryzae*-produced silver nanoparticles with different antibiotics and essential oils derived from *Cupressus sempervirens* and *Asteriscus graveolens* (Forssk). Trop J Pharm Res. 2019;18(12):2605-16. doi: 10.4314/tjpr.v18i12.21.
33. Moteriya P, Padalia H, Chanda S. Characterization, synergistic antibacterial and free radical scavenging efficacy of silver nanoparticles synthesized using *Cassia roxburghii* leaf extract. J Genet Eng Biotechnol. 2017;15(2):505-13. doi: 10.1016/j.jgeb.2017.06.010.
34. Durán N, Nakazato G, Seabra AB. Antimicrobial activity of biogenic silver nanoparticles, and silver chloride nanoparticles: an overview and comments. Appl Microbiol Biotechnol. 2016;100(15):6555-70. doi: 10.1007/s00253-016-7657-7.
35. Khleifat KM, Matar SA, Jaafreh M, Qaralleh H, Al-Limoun MO, Alsharafa KY. Essential oil of *Centaurea damascena* aerial parts, antibacterial and synergistic effect. J Essen Oil Bear Plants. 2019;22(2):356-67. doi: 10.1080/0972060x.2019.1626292.
36. Padalia H, Moteriya P, Chanda S. Green synthesis of silver nanoparticles from marigold flower and its synergistic antimicrobial potential. Arab J Chem. 2015;8(5):732-41. doi: 10.1016/j.arabjc.2014.11.015.
37. Sezik E, Yeşilada E, Honda G, Takaishi Y, Takeda Y, Tanaka T. Traditional medicine in Turkey X. Folk medicine in central Anatolia. J Ethnopharmacol. 2001;75(2-3):95-115. doi: 10.1016/s0378-8741(00)00399-8.
38. Massa N, Cantamessa S, Novello G, Ranzato E, Martinotti S, Pavan M, et al. Antifungal activity of essential oils against azole-resistant and azole-susceptible vaginal *Candida glabrata* strains. Can J Microbiol. 2018;64(10):647-63. doi: 10.1139/cjm-2018-0082.
39. Jain N, Bhargava A, Majumdar S, Tarafdar JC, Panwar J. Extracellular biosynthesis and characterization of silver nanoparticles using *Aspergillus flavus* NJP08: a mechanism perspective. Nanoscale. 2011;3(2):635-41. doi: 10.1039/c0nr00656d.
40. Joanna C, Marcin L, Ewa K, Grażyna P. A nonspecific synergistic effect of biogenic silver nanoparticles and biosurfactant towards environmental bacteria and fungi. Ecotoxicology. 2018;27(3):352-9. doi: 10.1007/s10646-018-1899-3.
41. Ghosh S, Patil S, Ahire M, Kitture R, Kale S, Pardesi K, et al. Synthesis of silver nanoparticles using *Dioscorea bulbifera* tuber extract and evaluation of its synergistic potential in combination with antimicrobial agents. Int J Nanomedicine. 2012;7:483-96. doi: 10.2147/ijn.s24793.
42. Zhang W, Pu Z, Du S, Chen Y, Jiang L. Fate of engineered cerium oxide nanoparticles in an aquatic environment and their toxicity toward 14 ciliated protist species. Environ Pollut. 2016;212:584-91. doi: 10.1016/j.envpol.2016.03.011.
43. Chernousova S, Epple M. Silver as antibacterial agent: ion, nanoparticle, and metal. Angew Chem Int Ed Engl. 2013;52(6):1636-53. doi: 10.1002/anie.201205923.
44. Zhang X, Yan S, Tyagi RD, Surampalli RY. Synthesis of nanoparticles by microorganisms and their application in enhancing microbiological reaction rates. Chemosphere. 2011;82(4):489-94. doi: 10.1016/j.chemosphere.2010.10.023.
45. Lee SH, Jun BH. Silver nanoparticles: synthesis and application for nanomedicine. Int J Mol Sci. 2019;20(4):865. doi: 10.3390/ijms20040865.